State Feedback Controller Based on Bond Graph Observers

Attafi Rim† and Zanzouri Nadia††,

† University of Tunis El Manar, Faculty of Sciences of Tunis
LR11ES20, Analysis Conception and Control of Systems Laboratory-ENIT,
Box 37, Le Belvedere 1002, Tunis, Tunisia
†† University of Tunis, Preparatory Engineering Institute of Tunis,
2 Rue Jawher Lel Nahrou Monfleury, 1089 Tunis, Tunisia

Summary
This paper presents a comparative study between two techniques in order to outline the stability performances of the string tension racket of stringing machine, when we apply the state feedback controller. These two techniques are the graphic approach which based on Bond Graph (BG) tool, and the optimization method LMI (Linear Matrix Inequality). Therefore, in this paper, we will take into account the advantage of using the two techniques in designing the Luenberger (full order and reduced order) and the functional observers in closed loop for estimation and control purposes. The simulation and experimental results are presented and discussed.

Key words:
Stringing machine, state feedback controller, BG tool, LMI.

1. Introduction

The linear time invariant systems stabilization by the state feedback controller via the pole placement technique can be performed at the real time by the Luenberger observer [1], Kalman filter [2] and at the frequency time [3].
Many techniques exist in the literature for the calculation of the state feedback controller gain as well as the observer gain. We found the pole placement technique [4] which placed arbitrarily the eigenvalues of the systems, and the optimization method as LMI (Linear Matrix Inequality) [5] and BMI (Bilinear Matrix Inequality) [6], which gives an exactly location in the complex plan.
Few works relative to the state feedback stabilization in the graphic case, which based on the BG approach. Indeed, [7] applied the control on the Luenberger observer. In this case, the control gain determined by the causal path calculus [8] as well as the Luenberger observer gain [9].
Therefore, in this paper, we will take into account the advantage of using the BG approach, in designing the Luenberger and the functional observers for estimation and control purposes. The paper also highlights and clarifies the need for the optimization method LMI (Linear Matrix Inequality), to outline the stability performances.
In summary, this paper is organized as follows: Section 2 presents the methodology of BG modeling. Section 3 describes the studied system. Section 4 deals with observers design based on algebraic and graphic methods. We simulate the error evolution and the control strategies, and we discuss the simulation and the experimental results in section 5. Section 6 concludes the paper.

2. The Methodology of BG Modeling

To study the control laws, the step of modeling is indispensable. Despite its multidisciplinary projects, the BG was hyped up. It's created in 1961 by [10] and developed by [11]. The BG is a tool of modeling in various fields (electrical, mechanical, hydraulic...). It's based on power transfer between the different parts of the systems. To describe the systems dynamic, there are two pairs of variables, effort symbolized as e and flow symbolized as f, the product of which constitutes the power. There are also the energy variables, which are the generalized momentum p (time integral of effort) and the generalized displacement q (time integral of flow). The classification of BG elements is as follows; the passive elements as inertial elements (I), capacitive elements (C) and resistive elements (R). The effort sources (S_e) and flow sources (S_f) are the active elements. Two ports elements represented by transformer elements (TF) and gyrator elements (GY), and multi ports elements represented by effort junctions (J_0) and flow junctions (J_1).
Despite BG approach applicability to the architecture and the design of the observer [12, 13], yet it has used as a tool for modeling [14], diagnosis [15] and for fault tolerant control synthesis [16].
Note that the graphical formalism is used in this paper for modeling, simulation and practice purposes.

3. Stringing Machine BG Model

In the following section, an application in real system is provided to demonstrate the effectiveness of the proposed

Manuscript received April 5, 2018
Manuscript revised April 20, 2018

methods. The studied system Fig. 1 is composed of two zones; the cradle and the clamp, and the tensioning mechanism. The first zone corresponds to the manual operations, which might be attached to the racket, and keeps respective the rope tension. The second zone, is automated which allows to obtain the precise rope tension.

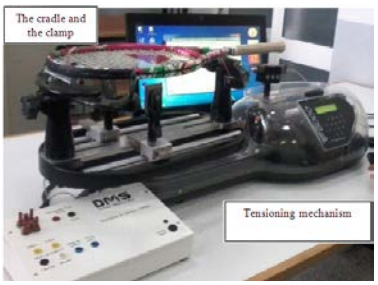

Fig. 1 The stringing machine (laboratory test)

The word BG of the stringing machine in open loop is composed of four blocks Fig. 2, the first one presents the DC motor, the second presents the reducer, the third block gathers the gable and the chain, the spring the trolley and the rope are presented in the fourth block.

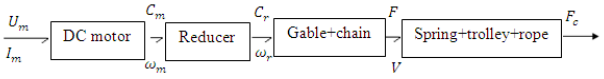

Fig. 2 Word BG of stringing machine

The detailed BG model of the system is depicted in Fig. 3. In fact, the DC motor is used to associate the physical phenomenon or components considered by the induced current I_m, and by the mechanic part which depends on the rotation speed of its axe. Whether, U_m is the induced tension, R_m is the resistance, L_m is the inductance, R_1 is the resistive viscous friction, and J_m is the moment of the rotor inertia and the shaft of inertial type. The gyrator element has as r_1 constant, and transforms the electromotive force into rotation speed of the reducer tree. The compressibility of the tree is presented by C_1 element. The third block transforms the rotation movement into translation movement via winding up the rope which is presented as the transformer element witch has as r_2 constant. The mass of the chain is given by m and the frictions at the gable are negligible. We consider that the tree is of elastic type (whether $C_2 = \frac{K_r}{1 + K_r/K_c}$ (K_r is the spring stiffness and K_c is the rope stiffness), the loss resistance is given by R_2). The mass of the trolley is negligible.

From Fig. 4, we can deduce the gear motor equations:

$$U_{L_m} = U_m - U_{R_m} - U_e \tag{1}$$

$$U_{R_m} = R_m I_m$$

$$p_{L_m} = \int U_{L_m} dt$$

$$U_e = r_1 \omega_m$$

$$U_{e_m} = r_1 I_m$$

$$F_{J_m} = U_{e_m} - F_{R_1} - C_m \tag{2}$$

$$F_{R_1} = R_1 \omega_m$$

$$p_{J_m} = \int F_{J_m} dt$$

$$\omega_r = \omega_m - \omega_2$$

The gable + chain equations:

$$F_{pig} = 1/r_2 C_r \tag{3}$$

$$\omega_r = 1/r_2 V_1$$

$$F_{ch} = F_{pig} - F_{mo}$$

$$p_m = \int F_{ch} dt$$

And the spring + trolley + rope equations:

$$V_{K_T} = V_3 - V_4 \tag{4}$$

$$F_{K_T} = \psi_{C_2}(\int V_{K_T} dt)$$

$$q_{C_2} = \int V_{K_T} dt$$

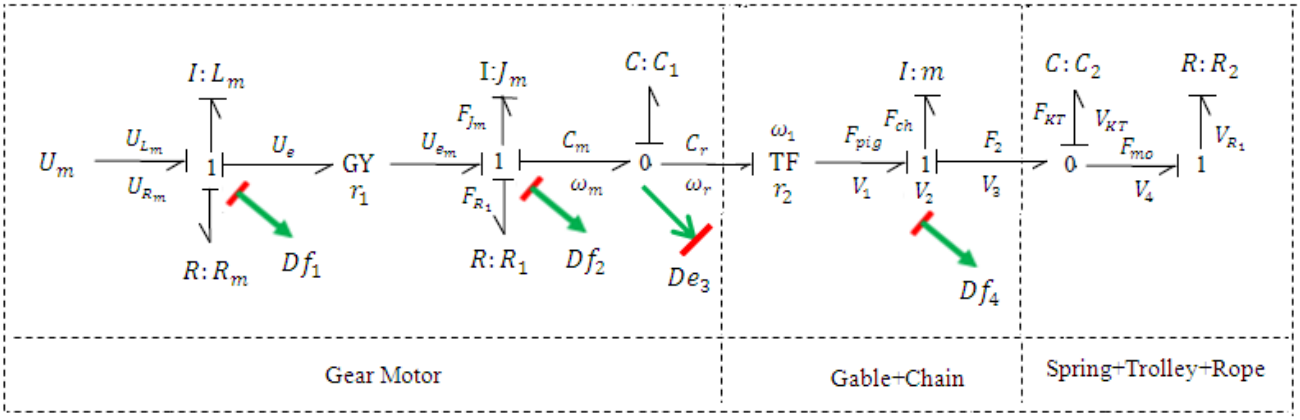

Fig. 3 BG model of stringing machine

From the BG model and the equations above, we can deduce the state space of the system described by equation (5):

$$\begin{cases} \dot{x} = Ax + Bu \\ y = Cx \end{cases} \tag{5}$$

With $x = \lfloor p_{Lm} \quad p_{Jm} \quad q_{C1} \quad p_m \quad q_{C2} \rfloor^t$ is the state vector, $y = \lfloor D_{f1} \quad D_{f2} \quad D_{e3} \quad D_{f4} \rfloor^t$ is the measured output variables, $u = U_m$ is the control input variable and the system matrices A, B and C are

$$A = \begin{pmatrix} -R_m/L_m & -r_1/J_m & 0 & 0 & 0 \\ r_1/L_m & -R_1/J_m & -1/C_1 & 0 & 0 \\ 0 & 1/J_m & 0 & -1/m r_2 & 0 \\ 0 & 0 & 1/C_1 r_2 & 0 & -1/C_2 \\ 0 & 0 & 0 & 1/m & 0 \end{pmatrix}$$

$$B = \begin{pmatrix} 1 \\ 0 \\ 0 \\ 0 \\ 0 \end{pmatrix} \text{ and } C = \begin{pmatrix} 1/L_m & 0 & 0 & 0 & 0 \\ 0 & 1/J_m & 0 & 0 & 0 \\ 0 & 0 & 1/C_1 & 0 & 0 \\ 0 & 0 & 0 & 1/m & 0 \end{pmatrix}$$

The characteristics of the parameters are listed in the Table 1.

Table 1: Parameters of the stringing machine

Symbol	***Designation***	***Nominal values***
R_m	Rotor resistance	1.1Ω
L_m	Rotor inductance	$1mH$
J_m	Moment of geared motor	$0.05Kg.m^2$
R_1	Coefficient of viscous	$0.28N.m/rad/S$
r_1	Coefficient of torque	$0.0386N.m/A$
r_2	Reduction ratio	$0.01N.m/A$
m	Chain mass	$0.3Kg$
K_r	Spring stiffness	$4N/mm$
K_c	Rope stiffness	$32.7N/mm$
C_1	Coefficient of compressibility	10^{-4}
C_2	Coefficient of compressibility	0.00028
R_2	Loss resistance	$1000N.m/rad/S$

According to [17], any system driven by the output of the given system can serve as an observer for that system.

4. Observer Design for State Feedback Control

4.1 Analytical Observers Design

4.1.2 Full Order Luenberger Observer

The aim of the full observer is to estimate all its states. The observer-based controller structure is defined as

$$\begin{cases} \dot{\hat{x}} = (A - B K_{feedback})\hat{x} + B K_{forward} y_c + G(y - \hat{y}) \\ \hat{y} = C\hat{x} \end{cases} \quad (6)$$

Where $x \in R^n$, $y \in R^p$, $u \in R^m$, $K_{feedback}$ is the feedback gain matrix, y_c is the reference input, $K_{forward}$ is the forward gain matrix and G is the observer gain to be determined. The estimation error is $e = x - \hat{x}$ leading to $\dot{e} = (A - GC)e$.

4.1.2 Reduced Order Luenberger Observer

This observer is designed to estimate the remaining part of the state vector, that is $\hat{x}_b$ of dimension $(n-p)$. The aim of the reduced order observer is to separate the state vector of (5) in non-estimated variables noted x_a and estimated variables noted x_b. The reduced observer structure is given by

$$\begin{cases} \dot{z} = \overline{M}\hat{z} + \overline{N}u + \overline{P}y \\ \hat{x}_b = z + \overline{L}y \end{cases} \quad (7)$$

With z is auxiliary variable which avoid the time derivation of the output, when we calculate the estimated state.

$$\overline{M} = \overline{A}_{bb} - \overline{L}\,\overline{A}_{ab} \quad (8)$$

$$\overline{N} = \overline{B}_b - \overline{L}\,\overline{B}_a \quad (9)$$

$$\overline{P} = \overline{A}_{ba} + \overline{A}_{bb}\overline{L} - \overline{L}\,\overline{A}_{aa} - \overline{L}\,\overline{A}_{ab}\overline{L} \quad (10)$$

$\overline{L} \in \Re^{(n-m)m}$ is the observer gain matrix.

$\overline{A}_{aa} = (C_a A_{aa} + C_b A_{ba}) C_a^{-1}$, $\overline{A}_{ab} = (C_a A_{ab} + C_b A_{bb} - \overline{A}_{aa} C_b)$, $\overline{A}_{ba} = A_{ba} C_a^{-1}$, $\overline{A}_{bb} = A_{bb} - A_{ba} C_a^{-1} C_b$

$\overline{B}_a = C_a B_a + C_b B_b$ and $\overline{B}_b = B_b$ are the sub-matrices of the state matrix.

The observer-based controller structure is given by

$$\begin{cases} \dot{z} = \overline{M}\hat{z} + \overline{N}(K_{forward} y_c - K_{feedback} x) + \overline{P}y \\ \hat{x}_b = z + \overline{L}y \end{cases} \quad (11)$$

The dynamic of the estimation error is defined as $e = x_b - \hat{x}_b$ leading to $\dot{e} = (\overline{A}_{bb} - \overline{L}\,\overline{A}_{ab})e$.

4.1.3 Functional Observer

The aim of the functional observer is to estimate directly the control law $(W = Kx)$ with $W \in R^r$, where $r \le n$ without estimating all its states. We assume that the pair (A, C) is observable and $rankC = p$ and $rankK = r$. Let us propose that $C = (I \quad 0)$ and $K = (K_a \quad K_b)$. So we obtain $x_a = y$ and $x_b = K_b^{-1}(W - K_a y)$.

After some algebraic manipulations, the linear functional observer has the following form:

$$\begin{cases} \dot{\hat{z}} = (A_{bb} - L A_{ab})\hat{z} + (A_{ba} - L A_{ab} L - L A_{aa} + A_{bb} L)y + (B_b - L B_a)u \\ \hat{W} = K_b \hat{z} + (K_a + K_b L)y \end{cases} \quad (12)$$

With L is the observer gain matrix to be determined.

In the general case, the form of the observer structure is as follows:

$$\begin{cases} \dot{\hat{z}} = E\hat{z} + Dy + Hu \\ \hat{W} = P\hat{z} + Fy \end{cases} \quad (13)$$

With

$$E = A_{bb} - L A_{ab},\ D = A_{ba} - L A_{ab} L - L A_{aa} + A_{bb} L,\ H = B_b - L B_a,\ P = K_b,\ F = K_a + K_b L \quad (14)$$

The dynamic of the estimation error is defined as

$$e = W - Kx = z - Tx \quad (15)$$

Assumptions :

$\hat{W}$ in (12) is an asymptotic estimate of W for any x_0, $\hat{W}_0$ and any u, if and only if the following assumptions are satisfied:

1. E is a Hurwitz matrix, i. e., has all its eigenvalues in the left-hand side of the complex plane.
2. $TA - ET = DC$
3. $PT + FC = K$ (16)

4. $H = TB$

Where T is a constant matrix, as $\lim_{t\to\infty}(z - Tx) = 0$ Then the estimation error dynamics are written as:

$$\dot{e} = Ee \tag{17}$$

Using the linear state-space system representation and linear algebra, we have introduced the Luenberger and the functional observers for the state vector and the state vector function estimations. To simplify some classical matrices calculations, the observers design based on BG approach will be presented.

4.2 BG Observers Design Model

The present section introduces the procedure to design a Luenberger and functional observers using the bond graph tool [18]. The algorithm is formulated as follows:

Step 1: Checking the redundant outputs

The property of existence of redundant outputs, summarized in the bond-graph rank (bg-rank), which can confirm the rank of the model's matrices. Indeed, the $bg - rank[C]$ is equal to the number of detectors in a model that can be dualized without creating causality conflicts. So, the $bg - rank[C]$ will be equal to the number of non-redundant outputs; $bg - rank[C] = p$

Step 2: Investigating the structural observability of the system BG model

With reference to [19]'s theorem, a bond graph model is structurally observable if and only if the below conditions are satisfied:

When we put the BG model of the system with preferred integral causality, there is a causal path linking the sensors for each dynamic element I or C.

When the BG model of the system is affected with derivative causality, all the element I or C .have derivative causalities and the sensors are dualized.

The design of the observers bond graph models steps are as follows:

4.2.1 Full Order Luenberger Observer

Step 1 and step 2 (see above).

Step 3: Linear output injection: Addition of the term $G_i(y - \hat{y})$ in the dynamical elements of the observer model.

The observer BG model in closed loop is given by Fig. 4 :

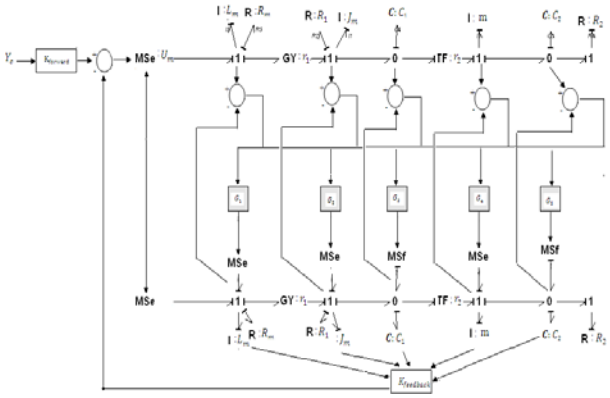

Fig.4 Full observer BG model in closed loop

4.2.2 Reduced Order Luenberger Observer

Step 1 and step 2 (see above).

To avoid C_a^{-1} calculus, and to simplify the reduced order observer design, [9] uses the bicausality concept. The procedure of reduced observer design summarizes by the following steps:

Step 3: Selection of x_a,verification that $bg\_rank[C] = p$ (invertibility) and calculation of C_a and C_b.

Step 4: Suppression of the dynamical elements associated with x_a.

Step 5: Sum of the term $\bar{L}y$

Step 6: Sum of the term $\phi = -\bar{L}(\overline{A}_{aa} y + \overline{A}_{ab}(\hat{z} + \bar{L}y) + \overline{B}_a u)$

Applying the step above, the BG model of the reduced observer in closed loop is presented in Fig. 5.

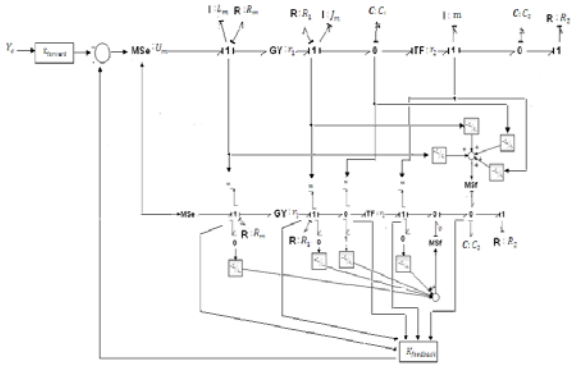

Fig. 5 Reduced observer BG model in closed loop

4.2.3 Functional Observer

Step 1 and step 2 (see above).

Step 3: Selection of X_a: From the BG point of view, the non-estimable variables in BG model are the state variables associated to the dynamical elements which are connected directly to the detectors by a causal path or through the R element.

Step 4: Change of X_a causality: We change the causality of the dynamical elements associate with X_a which is made from the initial BG model into a derivative causality, as shown in Fig. 6.

Step 5: Injection of the term Fy: As in the case of the full order observer design, we consider the term Fy as an error signal which comes from an extra junction on the effort or flow source bond via an active bond, and injected it on the dynamical elements associated to the state variable, which has a linear function with the control variable by the modulated source, as shown in Fig. 7.

Step 6: Sum of the term P: In the observer BG model, the term P is added with a modulated source. Indeed, it's the flow when the control variable is associated to the C element (and it's the effort when the control variable is associated to the I element), as shown in Fig. 8.

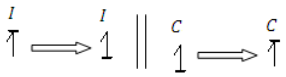

Fig.6 Derivative causality of the elements associated with X_a

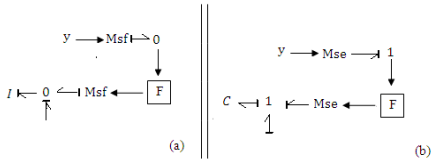

Fig. 7 Fy injection to: (a) I element, (b) C element

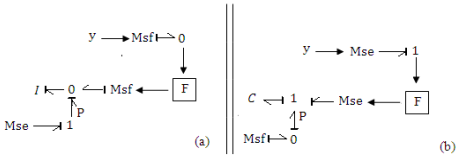

Fig. 8. Addition of the term P in the observer BG model: (a) I element, (b) C element

Applying the step above, the functional observer BG model shown in Fig.9

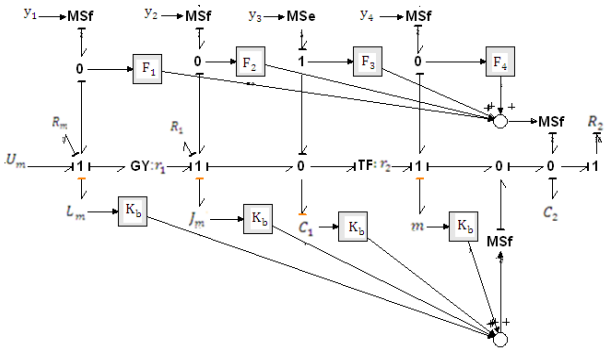

Fig. 9 BG model of the functional observer

Thereafter, we compute the observer gain via both BG and LMI methods.

4.2.4 Observer Gain Computing

4.2.4.1 By BG Method

The observer gains G, $\bar{L}$ and L can be computed using two different methods. The first consists in the traditional methods using the state equations calculation from the system bond graph model. The second is based on the formal calculation of the characteristic polynomial $P_{(A-GC)}(s)$, $P_{(\bar{A}_{aa}-\bar{L}\bar{A}_{ab})}(s)$ and $P_{(A_{bb}-LA_{ab})}(s)$ respectively. It uses the causal manipulations and structural properties on the bond graph model without any calculations using [8]'s theorem cited below

The value of each coefficient of the characteristic polynomial

$$P_A(s) = s^n + \alpha s^{n-1} + \ldots + \alpha_{n-1}s + \alpha_n \qquad (18)$$

equal to the constant term (without the Laplace operator) of the total gain of the families of causal cycles of order i in the bond graph model. The gain of each family of causal cycles must be multiplied by $(-1)^d$ if the family consists of d disjoined causal cycles.

Thus, the causal analysis to calculate the observer gains is made only with the family of causal cycles in the observer's bond graph.

4.2.4.1 By LMI Method

The decay rate is strictly upper to α, if there exist a Lyapunov function $V(x)$, for all $x \neq 0$, $V(x) \text{ f } 0$ and $\dot{V}(x) = -2\alpha V(x)$.

We choose $V(x) = x^T Px$ with P is a symmetric matrix will be determined, [5].

$$\begin{cases} V(x) > 0 \\ \dot{V}(x) < -2\alpha V(x) \end{cases} \Leftrightarrow \begin{cases} P > 0 \\ A^T P + PA + 2\alpha P < 0 \end{cases} \Leftrightarrow \begin{cases} P > 0 \\ (A+\alpha I)^T P + P(A+\alpha I) < 0 \end{cases} \quad (19)$$

The Luenberger (full and reduced) and the functional observers gain matrices are computed through the solution of the following inequalities [5]:

$$\begin{cases} P > 0 \\ (A+\alpha I)^T P + P(A+\alpha I) - C^T Z^T - ZC < 0 \end{cases} \quad (20)$$

$$\begin{cases} P > 0 \\ (\overline{A}_{bb}+\alpha I)^T P + P(\overline{A}_{bb}+\alpha I) - (\overline{A}_{ab})^T Z^T - Z(\overline{A}_{ab}) < 0 \end{cases} \quad (21)$$

$$\begin{cases} P > 0 \\ (A_{bb}+\alpha I)^T P + P(A_{bb}+\alpha I) - (A_{ab})^T Z^T - Z(A_{ab}) < 0 \end{cases} \quad (22)$$

Where P is a symmetric, positive and defined matrix, and α is the decay rate of the observer.

For every P and Z satisfying the LMIs inequalities, it corresponds to stabilizing observers.

Solving the (20), (21) and (22) LMIs inequalities, the observer gains can be performed using the following expression:

$$G = P^{-1}Z \quad (23)$$

$$\overline{L} = P^{-1}Z \quad (24)$$

$$L = P^{-1}Z \quad (25)$$

The closed-loop system of (5) is quadratically stable, if and only if the following LMI are feasible:

$$\begin{cases} P > 0 \\ (A-BK_{feedback})^T P + P(A-BK_{feedback}) + 2\alpha P \le 0 \end{cases} \quad (26)$$

Where P is a symmetric, positive and defined matrix, and α is the decay rate.

The controller design is the result of the following LMI problem, where Q is a symmetric, positive and defined matrix

$$\begin{cases} Q > 0 \\ (A+\alpha I)Q + Q(A+\alpha I)^T + BY + Y^T B^T < 0 \end{cases} \quad (27)$$

The resulting controller feedback gain is given by:

$$K_{feedback} = -YP \quad (28)$$

Where Y and P are the solutions, such that LMI problem given by (26) is feasible.

The forward control gain $K_{forward}$ computed such as $y_c(t)$ equal to the reference input. To ensure that $\lim_{t\to\infty} y(t) = y_c(t)$. So,

$$K_{forward} = \frac{1}{C(-A+BK_{feedback})^{-1}B} \quad (29)$$

5. Simulation and Experimental Results

5.1 Simulation Results

To determine the observer's gains a pole placement technique is used. Each observer gain is represented as follows:

$$G = \begin{pmatrix} -1 & 0 & 0 & -26000 \\ 0 & 0 & -1 & 0 \\ 0 & 1 & 1 & -110 \\ 107 & 0 & 100 & -160 \\ -1 & 0 & 0 & -1190 \end{pmatrix} \quad (30)$$

$$\overline{L} = 10^5 [0 \quad 0 \quad 0 \quad -2.4] \quad (31)$$

- By BG method :

Applying [8]'s theorem in the BG functional observer model (Fig. 9), we found one order causal cycle. Then, selecting α_1 as the desired coefficient of the characteristic polynomial:

$$P_{(A_{bb-L}A_{ab})}(s) = s + \alpha_1 \quad (32)$$

The calculus of L is directly derived from $\alpha_1$because

$$\alpha_1 = -\frac{F_4}{C_2} = -\frac{(K_a + K_b L_4)}{C_2} \tag{33}$$

Then, L_4 is calculated from (33)

$$L_4 = -\frac{(\alpha_1 C_2 + K_a)}{k_b} \tag{34}$$

So, the functional observer gain is

$$L = 10^4 [0 \quad 0 \quad 0 \quad -1.04] \tag{35}$$

As the system is controllable, a linear state feedback control law can be easily derived with pole placement technique. Then,

$$K_{feedback} = 10^7 [0 \quad 0.1 \quad -487 \quad -1.8 \quad 1] \tag{36}$$

$$K_{forward} = 10^3 [-7.98 \quad 0 \quad 0 \quad 0] \tag{37}$$

- By LMI method :

$$G_{(lmi)} = \begin{pmatrix} -10 & -1730 & -5010 & -10 \\ 40 & 7430 & -10 & -680 \\ 50110 & -69100 & 10 & 3070 \\ 0 & 110 & 14940 & 44940 \\ 0 & 0 & 3620 & -138420 \end{pmatrix}, \alpha = 10^3 \tag{38}$$

$$\overline{L}_{(lmi)} = 10^5 (0 \quad 0 \quad 0 \quad -2.66), \ \alpha = 10 \tag{39}$$

$$L_{(lmi)} = 10^4 (0 \quad 0 \quad 0 \quad -8.72) \ \alpha = 10^3 \tag{40}$$

$$K_{feedback(lmi)} = 10^5 [8.98 \quad 0.039 \quad -0.0001 \quad 0.0015 \quad 0], \ \alpha = 10^4 \tag{41}$$

And

$$K_{forward(lmi)} = 10^5 [8.98 \quad 0 \quad 0 \quad 0] \tag{42}$$

To simulate the dynamic performance of the closed-loop system, a nonzero initial condition is required. The values of different system parameters are presented in Table 1. The control input $u(t)$ is a step signal start after $3s$ with amplitude of $^{100}m^3/s$. The gaussian noise amplitude equal to 0.25.

Before carrying out the simulation of different scenarios on the 20-SIM software, it is essential to validate the BG model (see Fig 10).

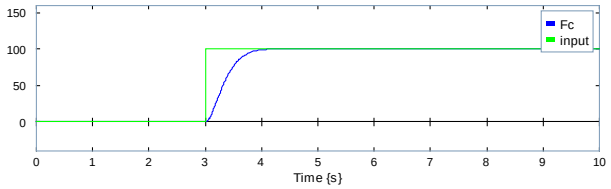

Fig. 10 Input and output (F_c) signals of the system

The output responses with pole placement and LMI techniques by full, reduced and functional observers are given in Figs. 11, 12, and 13 respectively.

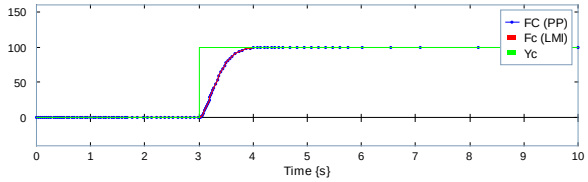

Fig. 11 String tension racket response (F_C) with pole placement and LMI techniques by full order observer

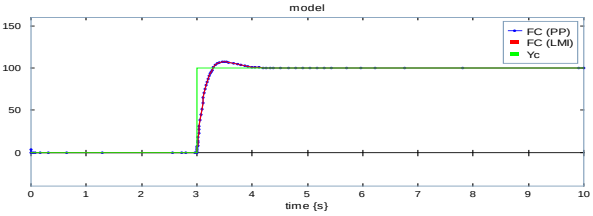

Fig. 12 String tension racket response (F_C) with pole placement and LMI techniques by reduced order observer

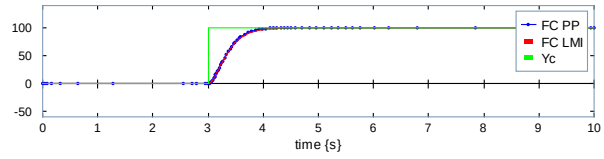

Fig. 13. String tension racket response (F_C) with pole placement and LMI techniques by functional observer

Now, the evolution of the estimation errors with pole placement (PP) and LMI technics, using the Luenberger and functional observers can be readily carried out (see Figs. 14, 15 and 16).

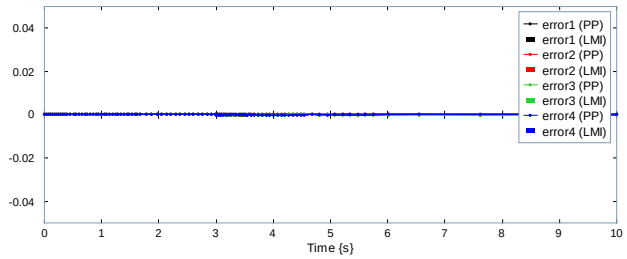

Fig. 14 Full order observer estimation error by pole placement (PP) and LMI techniques for the stringing machine

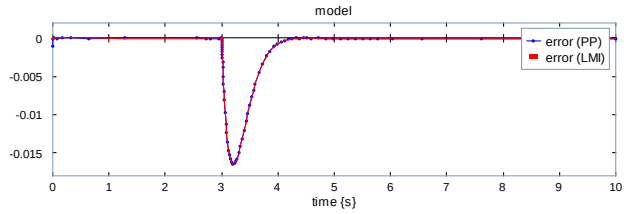

Fig. 15 Reduced order observer estimation error by pole placement (PP) and LMI techniques for the stringing machine

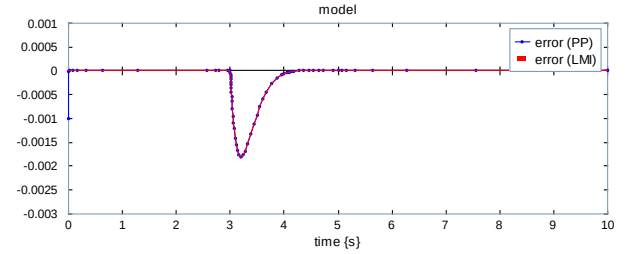

Fig.16 Functional observer estimation errors by pole placement (PP) and LMI techniques for the stringing machine

It's clear from the figures above, that the asymptotic convergence property of the Luenberger and functional observers have been attenuated.

5.1 Experimental Results

Until the robustness of the proposed system is targeted, many tests have been validated experimentally using a test bench (Fig. 1) around the response of the string tension racket. The experimental input and the output signals are shown in Fig.17. The experimental estimation errors evolutions of Luenberger and functional observers are presented in Figs. 18, 19 and 20 respectively.

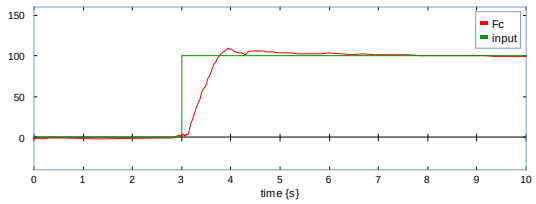

Fig.17 Experimental input and outputs signals obtained from the stringing machine.

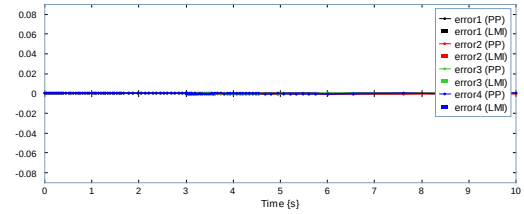

Fig.18 Experimental estimation error evolution of full observer

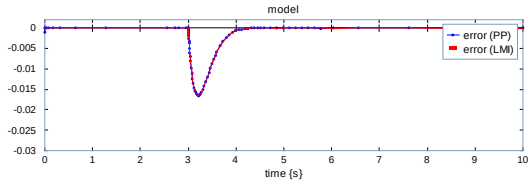

Fig.19 Experimental estimation error evolution of reduced observer

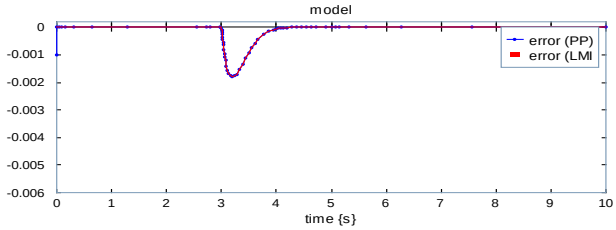

Fig.20 Experimental estimation error evolution of functional observer

The Table 2 presents the difference between the pole placement and LMI methods in terms of stabilization time and error.

Table 2: Observers characteristics

	Errors (%)		Stabilization time (s)	
Technics observer	Pole placement (PP)	LMI	Pole placement (PP)	LMI
Full observer	0.012%	$^{7}10^{-5}$ %	5.49*s*	1.46*s*
Reduced observer	4.74%	1.56%	6.43*s*	3*s*
Functional observer	1.96%	0.96%	3*s*	1.27*s*

As a result of these different scenarios, it seems clear that the simulation and experimental results are proven. We can see from the table, that LMI method is more accurate to use for our system because, it shows acceptable time of response and good stability. Besides, the pole placement technique has showed a longer time of stabilization than the LMI method.
The obtained control law ameliorates the rapidity and the accuracy of the system behaviour due to the proposed linear observers.

6. Conclusion

This paper has proposed the Luenberger and the functional observers designs based on BG approach. Two techniques BG and LMI are detailed. These two methods are applied on the same process, in order to improve the stability performances of the string tension racket of stringing machine. The study of Bond Graph (BG) method and Linear Matrix Inequality (LMI) suggest that the results of both techniques are very satisfactory in terms of rapidity, stability and precisions. But LMI method performs acceptable time of response and good stability. At the last particular attention will be paid to the study of the diagnosis based on BG Luenberger and functional observers in future research works.

Acknowledgments

The string machine considered in our work is available at the University of Tunis, Preparatory Engineering Institute of Tunis, 2 Rue Jawher Lel Nahrou Monfleury.

References

[1] D. P. Papadopoulos and A.K. Boglou “Pole-placement and model order reduction techniques applied to a hydro_unit_system for dynamic stability improvement,” J. Frank. Inst, vol. 325, pp.403-417,1988.
[2] J. L. Junkins and Y. Kim. Introduction to dynamics and control of flexible structures. American. Inst. Aeronau. Astro Inc. 370 l’Enfant Promenade, SW, Washington, DC 20024- 2518, 1993.
[3] J. M. Araujo, “Discussion on state feedback control with time delay,” Mechanical. Sys. Sign. Proce, vol. 98, pp. 368-370.
[4] C. A. Bin Karim and M. A. Zamee,“Design and analysis of pole placement controller for dynamic stability improvement of VSC-HVDC based power system,” 9th International Forum on Strategic Technology (IFOST), 21-23 oct, Cox’s Bzar, Bangladesh, 2014.
[5] G. Scorletti and G. Duc,“An LMI approach to decentralized H8 control,” Inter. J. Cont, vol. 74, pp. 211-224, 2001.
[6] W. Y. Chiu,“Method of reduction of variables for bilinear matrix inequality problems in system and control designs,” IEEE Trans. Syst. Man. Cyber. Syst, vol 47, pp. 1241-1256, 2017.
[7] G. A. Gilberto, R. Galindo, “Direct control in bond graph by state estimated feedback for mimo LTI systems,” IEEE International Conference on Control Applications, 18-20 Sept, Glasgow, Scotland, UK 2002.
[8] A. Rahmani, C. Sueur and G. Dauphin-Tanguy,“Pole assignment for systems modeled by bond graph,” J. Frank. Ins, vol. 331, pp. 299-312, 1994.
[9] C. Pichardo-Almarza, A. Rahmani G. Dauphin-Tanguy and M. Delgado,“Using the bicausality concept to build reduced order observers in linear time invariant systems modelled by bond graphs,” Proceedings of European Control Conference (ECC), 2003.
[10] H. M. Paynter. Analysis and Design of Engineering Systems. MIT Press, Cambridge-Massachusetts, 1961.
[11] D.C. Karnopp and R. C. Rosenberg. Systems Dynamics: a Unified Approach. John Wiley & Sons Inc, 1975.
[12] A. Sallami, N. Zanzouri and M. Ksouri,“Robust fault diagnosis observer of dynamical systems modeled by BG approach,” Inter. J. Comp. Scien. Netw. Security, vol. 12, pp. 120-125, 2012.
[13] E. Fathallah and N. Zanzouri,“Cement water treatment process hybrid BG modeling and robust diagnosis,” Inter. J. Comp. Scien. Netw. Security, vol. 17, pp. 13-25, 2017.
[14] N. Zitouni, B. Khiari, R. Andoulsi and A. Sellami, “Modelling and nonlinear control of a photovoltaic system with storage batteries: a bond graph approach,” Inter. J. Comp. Scien. Netw. Security, vol. 11, pp. 105-114, 2011.
[15] A. Sallami, A. Ben Chaabene and A. Sallami,“Robust fault diagnosis of a reverse osmosis desalination system modeled by Bond Graph approach,” Inter. J. Comp. Scien. Netw. Security, vol. 11, pp. 105-111, 2011.
[16] H. Najari, R. El Harabi. and M. N. Abdelkrim, “An active fault tolerant control strategy based on bond graph adaptive observers,” Inter. J. Comp. Appl, vol. 176, pp. 1-7, 2017.
[17] D. G. Luenberger, “Observing the state of a linear system,” IEEE Trans. Mili. Elect, vol. 8, pp. 74-80, 1964.
[18] D. Karnopp, “Bond graphs in control: physical state variables and observers,” J. Frank. Inst, vol. 308, pp. 221-234, 1979.
[19] C. Sueur and G. Dauphin-Tanguy,“Structural controllability and observability of linear systems represented by bond graph,” J. Frank. Ins, vol. 326, pp. 869-883, 1989.

Attafi Rim was born in Béja, Tunisia, on August, 16, 1986. She received master’s degree in electronic from Science University of Tunis, Tunisia 2012. She is currently working toward the Ph.D. degree in Laboratory on AnalysisDesign and Control of Systems (LACS), National Engineering School of Tunis (ENIT), University Tunis El Manar.

Zanzouri Nadia received the S.M and Ph.D degrees in electrical engineering from Engineering School of Tunisia (ENIT) in 1999 and 2003 respectively. She is currently an associate professor at Preparatory Engineering Institute of Tunisia and researcher at Laboratory ACS of ENIT. Her research interests include Bond Graph modeling, Robust Fault Detection and Isolation (FDI) and Fault Tolerant Control (FTC) for Dynamical Systems and Hybrid Systems